Since January 2020 Elsevier has created a COVID-19 resource centre with free information in English and Mandarin on the novel coronavirus COVID-19. The COVID-19 resource centre is hosted on Elsevier Connect, the company's public news and information website.

Environmental Research 194 (2021) 110665

Contents lists available at ScienceDirect

Environmental Research

journal homepage: www.elsevier.com/locate/envres

Phase-wise analysis of the COVID-19 lockdown impact on aerosol, radiation and trace gases and associated chemistry in a tropical rural environment

Chaithanya D. Jain *, B.L. Madhavan, Vikas Singh, P. Prasad, A. Sai Krishnaveni, V. Ravi Kiran, M. Venkat Ratnam

National Atmospheric Research Laboratory, Gadanki, 517 112, India

ARTICLE INFO

Keywords:
Covid-19
Lockdown
Air quality
Aerosol
Radiation
Trace gases
Chemistry

ABSTRACT

Phase-wise variations in different aerosol (BC, AOD, PM_1, $PM_{2.5}$ and PM_{10}), radiation (direct and diffused) and trace gases (NO, NO_2, CO, O_3, SO_2, CO_2 and CH_4) and their associated chemistry during the COVID-19 lockdown have been investigated over a tropical rural site Gadanki (13.5° N, 79.2° E), India. Unlike most of the other reported studies on COVID-19 lockdown, this study provides variations over a unique tropical rural environment located at a scientifically strategic location in the Southern Indian peninsula. Striking differences in the time series and diurnal variability have been observed in different phases of the lockdown. The levels of most species that are primarily emitted from anthropogenic activities reduced significantly during the lockdown which also impacted the levels and diurnal variability of secondary species like O_3. When compared with the same periods in 2019, short-lived trace gas species such as NO, NO_2, SO_2 which have direct anthropogenic emission influence have shown the reduction over 50%, whereas species like CO and O_3 which have direct as well as indirect impacts of anthropogenic emissions have shown reductions up to 10%. Long-lived species (CO_2 and CH_4) have shown negligible difference (<1%). BC and AOD have shown reductions over 20%. Particulate Matter (1, 2.5 and 10) reductions have been in the range of 40 to 50% when compared to the pre-lockdown period. The changes in shortwave downward radiation at the surface, diffuse component due to the scattering and diffuse fraction have been +2.2%, −4.1% and −2.4%, respectively, in comparison with 2019. In contrast with the studies over urban environments, air quality category over the rural environment remained same during the lockdown despite reduction in pollutants level. All the variations observed for different species and their associated chemistry provides an excellent demonstration of rural atmospheric chemistry and its intrinsic links with the precursor concentrations and dynamics.

1. Introduction

COVID-19 pandemic has been a catastrophe for mankind around the world. It has been first detected in Wuhan, China during late 2019 and has since spread to other countries across the globe. COVID-19 has induced unprecedented containment strategies to stop its spread. Lockdown of the cities or entire countries to restrict the people's movement has been one among them, which on the other hand temporarily resulted in air quality improvement (Nakada and Urban, 2020; Navinya et al., 2020; Sharma et al., 2020; Singh et al., 2020; Xu et al., 2020a). Two major sources of anthropogenic emissions viz., industrial set-ups and transport (public as well as private) have been restricted only to the essential services and that resulted in significant reduction of emissions. Globally China first started the lockdown to contain the spread followed by Japan, Singapore, South Korea, European countries, USA and other countries including India as the virus spread globalized (Jain and Sharma, 2020). India went to a complete lockdown starting on 25 March 2020 for 21 days (Phase I) and then extended the lockdown until the end of May in 3 additional phases namely, 15/04 to 03/05 (Phase II), 04/05 to 17/05 (Phase III) and 18/05 to 31/05 (Phase IV) (MHA, 2020). More details on India lockdown in Supplementary Table S3.

In the recent years air pollution has become a global concern and there are many negative impacts of air pollution on public health (Manisalidis et al., 2020). Most of the countries irrespective of their socio-economic status are facing the air quality management challenges. More often it is the tradeoff between development and environmental protection policies. Majority of the megacities around the world are

* Corresponding author.
E-mail address: chaithanya.jain@narl.gov.in (C.D. Jain).

https://doi.org/10.1016/j.envres.2020.110665
Received 13 August 2020; Received in revised form 23 November 2020; Accepted 19 December 2020
Available online 24 December 2020

reported to be having poor air quality levels (Gulia et al., 2015; Singh et al., 2020). On the other hand the health conditions associated with the air pollution have been reported to be conducive for the COVID-19 infection and its increased risk of severity (Bashir et al., 2020; Ogen, 2020) however more research is required to establish this relation (Pisoni and Van Dingenen, 2020). The lockdown due to COVID-19 crisis has provided a unique scenario to assess the impact of developmental and social economic activities on the air quality. Even though this scenario is completely temporary but has demonstrated its effect on air quality across the globe. For example, China in general reported to have poor air quality (Wang and Hao, 2012) in its megacities but many studies reported from China have shown the significant improvement in air quality during the COVID-Lockdown (Shi and Brasseur, 2020; Xu et al., 2020a, 2020b). Three major cities in the central China's Hubei Province, Wuhan, Jingmen and Enshi showed a major reduction in the emissions of pollutants and improvement in their Air Quality Index (AQI) by 32.2%, 27.7%, and 14.9%, respectively, during the lockdown period (Xu et al., 2020a, 2020b). In a more broader study taking data from 1641 China National Environmental Monitoring Centers across China, Shi and Brasseur (2020) have reported a decrease of 29 ± 22% and 53 ± 10% in $PM_{2.5}$ and NO_2 respectively and an increase of O_3 concentrations by a factor 2.0 ± 0.7. Similar study from Spain (Europe) reported a reduction of PM_{10} (28 to 31.0%), BC and NO_2 (45 to 51%) and an increase of O_3 (33 to 57%) in Barcelona (Tobías et al., 2020). Another study from Brazil (South America) has also shown the concentration decrease in NO (up to −77.3%), NO_2 (up to −54.3%), and CO (up to −64.8%) and contrastingly an increase of O_3 concentrations by ~ 30% over São Paulo (Nakada and Urban, 2020).

The lockdown effects on mega cities over Indian sub-continent have also been reported in many studies. In a comprehensive study over India, Singh et al. (2020) estimated the changes in the six criteria air pollutants during the full lockdown (25-March to 3-May) across India at 134 sites in different regions of India. They reported significant decline for $PM_{2.5}$ and PM_{10} (40–60%); NO_2 (40–70%) and CO (20–40%); mixed behavior for SO_2 and O_3. They found decline in $PM_{2.5}$, PM_{10} and NO_2 throughout the day whereas O_3 has been found to decrease during the day but increase in the night over Indo Gangetic Plain (IGP). Sharma et al. (2020) after analyzing the data from 22 cities covering different regions of India reported an overall 43%, 31%, 10%, and 18% reduction in $PM_{2.5}$, PM_{10}, CO, and NO_2 observed during lockdown period resulting in improvement of AQI by 44, 33, 29, 15 and 32% in north, south, east, central and western India, respectively. Another study covering five megacities of India; Delhi, Mumbai, Chennai, Kolkata, and Bangalore (Jain and Sharma, 2020) has also highlighted a statistically significant decline in all the pollutants except for O_3. The concentrations of $PM_{2.5}$, PM_{10}, NO_2 and CO have been declined by ~41, ~52, ~51 and ~28%, respectively, during the lockdown phase. One more study focusing on megacity Delhi also showed similar results with the reduction of PM_{10} and $PM_{2.5}$ as high as about 60% and 39% respectively (Mahato et al., 2020). Among other pollutants, NO_2 (~52%) and CO (~30%) have also been reduced over Delhi during-lockdown phase. About 40–50% improvement in AQI has been observed just after four days of start of the lockdown Phase I. Satellite based observations have also shown a significant reduction in the tropospheric NO_2 vertical column densities (VCDs), mainly over the urban areas of India (Biswal et al., 2020). Similar reductions in NO_2 and SO_2 are also reported by Ratnam et al. (2020) using satellite measurements covering complete India. Interestingly they also showed reduction of 50–60% in AOD over north part of India covering IGP region but significant increase over Central India and attributed this to the natural processes.

All these pollutants species are short-lived species and have a direct linkage to the traffic and other anthropogenic emissions. There are other studies (Le Quéré et al., 2020; Safarian et al., 2020) which have predicted a reduction in the emissions of long-lived greenhouse gas species (impact on climate change) like CO_2 by 7% for the year 2020 as a result of COVI19-Lockdown. Along with the reduction in emissions the meteorological parameters like boundary layer, temperature and humidity also play an important role in deciding the concentration variability of these species (Ratnam et al., 2020).

Most of the studies summarized above have concentrated on the quantitative effects of lockdown in urban environments considering the restriction of public and to the best of our knowledge there are no studies which focused on the impact of the COVID-19 lockdown over the rural environment in India. It should be noted that there are differences in the tropospheric chemistry of urban and rural environments (Harrison, 2018) which has intrinsic links with reactive species concentrations and dynamics. For example, O_3 levels are higher in rural areas than in cities because O_3 can be scavenged by the compounds (NO_x) by which it is also formed. This scavenging occurs more often in cities than in rural areas, because there is more NO in cities (National Research Council, 1992). Therefore, the impact of lockdown on O_3 chemistry in rural environments may be different when compared to the urban environment. Such differences in urban and rural environments motivated to look at the lockdown effects (in a tropical rural site Gadanki) on the quantitative changes in trace gases, greenhouse gases, aerosols, and surface radiation, their diurnal variability and their chemical reactivity. Some of the observed data sets have also been inter-compared with the satellite measurements for the same time period.

2. Site description, measurements and data sets

2.1. Observation site

NARL, situated at Gadanki (13.5° N, 79.2° E, 375 m amsl), specializes in atmospheric research on various topics starting from the surface to the ionosphere. A wide variety of sophisticated instruments used in atmospheric probing are collocated under the same strategic location (Jayaraman et al., 2010). Gadanki is a tropical rural site (Gadhavi et al., 2015; Jain et al., 2019; Ravi Kiran et al., 2018; Renuka et al., 2014) located far from urban influence in the Southern Indian peninsula. The site is nearer to the Eastern Ghats with ~100 km distance from Bay of Bengal coast. Two major metropolitan cities of southern India viz., Bengaluru and Chennai are at ~250 and ~150 km distance from the site, respectively. The outline map of the observation site is shown in Supplementary Fig. S1. While the site has minimal influence of the urban sources, there exist a significant number of paddy fields and animal husbandry around Gadanki. The activities of biomass burning of agricultural residue, wood burning, and forest fires are occasionally observed in the nearby villages (Jain et al, 2018, 2019). Moderate to heavy traffic on the adjacent highway (~500 m west of observation site, connecting Chittoor and Tirupati) with a considerable portion being heavy-duty trucks are common. Winds at the site are mostly north-easterly during the winter season (December-January-February) and, south-westerly and south easterly during the summer season (March–April-May) (Ratnam et al., 2008).

2.2. Measurement data

Trace gases (NO, NO_2, CO, O_3 and SO_2) have been measured by Trace Gas Analyzers; Green House Gases (CH_4 and CO_2) have been measured by a Cavity Ring-Down Spectrometer (CRDS), PM_1, $PM_{2.5}$ and PM_{10} have been measured by PM sensor, Black Carbon (BC) by Aethalometer. Radiation parameters (Global Horizontal Irradiance - GHI and Diffuse Horizontal Irradiance – DHI) have been obtained by Pyranometer and Aerosol Optical Depth (AOD) has been obtained by Sky Radiometer. Supplementary Table S1 lists the percentage availability of all the data sets (daily data) during different phases considered for the present study.

Detailed description of the instrumentation used in this study has been given in the supplementary section S1. Briefly it can be put here as; Trace gas analyzers use non dispersive absorption spectroscopy technique for the continuous measurements of the respective species, CRDS

is based on the adaptation of Lambert Beer law using an optical cavity to see the decay of the light in it. PM sensors use light scattering method and are able to detect the particles with aerodynamic diameter of 0.3–10 μm. They can infer the real time mass concentrations of PM_1, $PM_{2.5}$, PM_{10} based on the confidential proprietary algorithm (Kelly et al., 2017). Aethalometer works on the principle of measuring the attenuation of the transmitted light at seven wavelengths (viz., 370 nm, 470 nm, 520 nm, 590 nm, 660 nm, 880 nm and 950 nm) through a quartz fiber filter tape loaded with aerosol particles on it. Pyranometer is a thermopile based sensor used for the measurement of global radiation received from the sun. Pyranometer uses the Sun tracking system consisting of a shading ball assembly for the shortwave incoming radiation measurements. Sky radiometer is an automatic ground-based radiometer measuring the direct solar radiation at 1 min interval and diffuse sky radiance with a 1° field-of-view with respect to the Sun at 10 min interval. Both the direct and diffuse sky radiances are used to retrieve the aerosol optical depth at 5 wavelengths, viz., 400, 500, 675, 870 and 1020 nm. AOD is retrieved using the SKYRAD package (SKYRAD.PACK, version 5.0) as detailed in Nakajima et al. (1996).

All the above instruments have been calibrated against the NIST traceable standards following the recommended procedures. The calibration factors have been applied on the measured data to ensure the data quality before going ahead with the analysis and interpretation. A consolidated list of all the different instruments used in the present study along with the salient specifications and further references to get more details are given in Table 1.

Daily mean MODIS AOD at 550 nm (MOD08_D3 C6 Level 3) and OMI Tropospheric Column NO_2 (OMNO2d v003) over Gadanki region (12.5°-14.5°N, 78.5°-80.5°E) during 2019 and 2020 have been obtained from NASA's Giovanni portal (https://giovanni.gsfc.nasa.gov/).

2.3. Meteorological data

Meteorological parameters such as Temperature (T), Relative Humidity (RH), Wind Speed (WS) and Atmospheric Boundary Layer (ABL) height have been taken from ERA5 Global reanalysis data sets (Hersbach et al., 2020) with a grid resolution of 0.25° x 0.25° keeping Gadanki at the centre. The European Centre for Medium-Range Weather Forecasts (ECMWF) ERA-Interim reanalysis provides global atmospheric parameters covering the time period from 1979 to present with 1-h temporal resolution, ~31 km spatial resolution (0.25 ° × 0.25 °) and 137 vertical pressure levels with a top level at 0.01 hPa.

2.4. Data period and methodology

In this study, the data period has been considered from 1-February-2020 to 31-May-2020. However while calculating the pre-lockdown averages, only five weeks prior to start of the lockdown has been used in order to minimize the meteorological impacts as the transition from winter to summer season occurred during the same time at Gadanki. Therefore the time period categories used in this study fall as pre-lockdown (15/02 to 21/03) and lockdown Phase I (25/03 to 14/04), Phase II (15/04 to 03/05), Phase III (04/05 to 17/05), Phase IV (18/05 to 31/05) and whenever it is mentioned lockdown it means total lockdown period (25/03 to 31/05). Same period data sets from 2019 have been used for the inter-comparison with 2020 to better understand the variations. Data sets of 22–24 March have been excluded in the study to avoid the impacts of partial lockdown and relaxations (22 March had been a voluntary lockdown across India, whereas during 23–24 March there had not been any lockdown).

The percentage changes in 2020 for different atmospheric parameters when compared with 2019 have been calculated by taking the difference between the 2019 and 2020 in respective time periods (Pre-lockdown, Phase I, Phase I, Phase II and Phase IV). However for PM, data has not been available for 2019 and the changes have been calculated with respect to the pre-lockdown period. Diurnal variations of meteorological and atmospheric parameters have been compared (between 2019 and 2020) after taking the difference between pre-lockdown and lockdown period in the respective years.

3. Results

3.1. Meteorological parameters during lockdown

Fig. 1 (a) shows the mean diurnal variations of the meteorological parameters and their differences during pre-lockdown and lockdown taken from ERA5 data sets for the years 2019 and 2020. Diurnal variations show a strong influence of solar irradiation during the day time

Table 1
List of various instruments used for obtaining different atmospheric parameter measurements used in this study.

Instrument	Parameters Measured	Lower detection limit	Uncertainty range	Mesauremnt period (Data Availability)	Reference for further details on instrumentation
Trace Gas Analysers APOA 370 APNA 370 APMA 370 APSA 370 Horiba, Japan	O_3 NO, NO_2, NO_X CO SO_2	0.5 ppbv 0.5 ppbv 20 ppbv 0.5 ppbv	±5.0%	1-Feb to 31-May (2019 and 2020)	Horiba (2020)
Picarro CRDS Analyzer G2401 Picarro INC, USA	CO CO_2 CH_4	15 ppbv 50 ppbv 1 ppbv	±2.0%	1-Feb to 31-May (2019 and 2020)	Picarro (2020)
PM sensor Plantower PMS 7003 Beijing Plantower Co. Ltd.	PM_1, $PM_{2.5}$ and PM_{10}	±10–15 μg/m^3	±10%	1-Feb to 31-May (2020)	Zheng et al. (2018)
Aethalometer AE31 Magee Scientific USA	Black Carbon (BC)	0.1 μg/m^3	±5.5%	1-Feb to 31-May (2019 and 2020)	Hansen (2005)
Sky Radiometer POM-01L Prede Co. Ltd, Japan	AOD	NA	±5.5%	1-Feb to 31-May (2019 and 2020)	Prede (2020)
Pyranometer CMP22 Kipp&Zonen, Netherlands	Global Horizontal Irradiation (GHI) and Diffuse Horizontal Irradiance (DHI)	NA	±1.5%	1-Feb to 31-May (2019 and 2020)	Kipp and Zonen (2020)

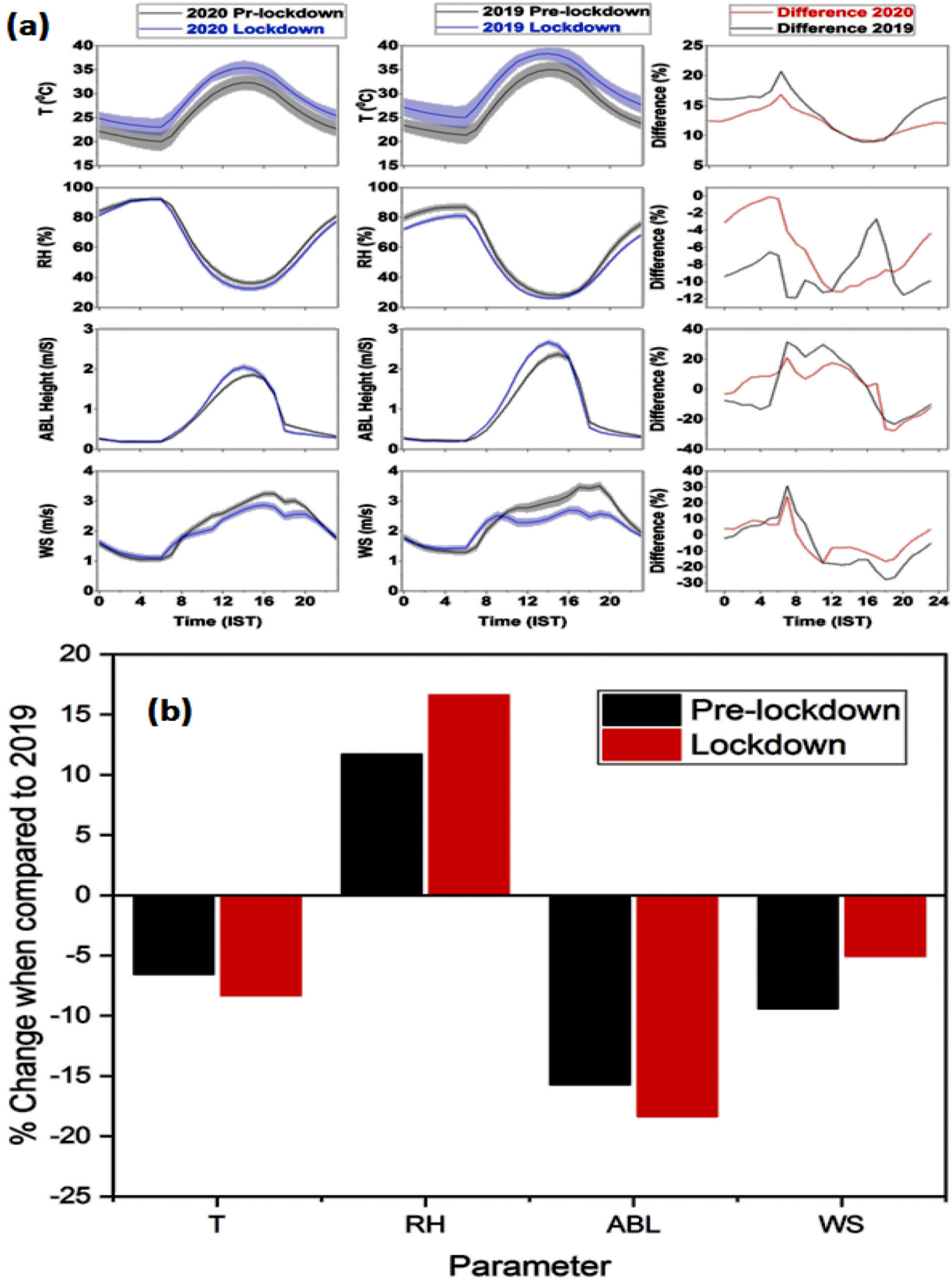

Fig. 1. (a) Diurnal variations of the meteorological parameters (averaged) at Gadanki obtained from ERA5 for the pre-lockdown (15/02 to 21/03) and lockdown (25/03 to 31/05) periods for 2019 and 2020. Differences represent the changes between the pre-lockdown and lockdown periods for the corresponding years. Shaded area represents the standard error. (b) Changes in the pre-lockdown and lockdown when compared to 2019.

(typical for a tropical hot and humid rural location). As a result Temperature (T), Wind Speed (WS) and Atmospheric Boundary Layer (ABL) height all show the daily maximum (late in the afternoon ~16:00 IST) whereas, Relative Humidity (RH) shows the daytime minimum and night time maximum. The diurnal variation in temperature follow similar variations during the pre-lockdown and lockdown periods in 2019 and 2020 except in 2020 night time temperature during the lockdown period has been cooler compared to 2019. ABL evolution too followed similar trends like T, however 2019 ABL evolution in the morning has been much sharper and the peak ABL height has been higher than 2020. ABL height has been comparatively higher during the lockdown period in both the years which is the result of higher temperatures compared to pre-lockdown period. This higher ABL height would contribute to the reduction in surface concentrations of aerosols and trace gases besides the local emissions. WS showed the minimal difference in its diurnal variation when compared between 2019 and 2020. Diurnal variation in RH during 2020 showed increase in both pre-lockdown and lockdown periods. In 2019, between the pre-lockdown and lockdown, there has been constant negative bias (owing to the diurnal temperature increase from pre-lockdown to lockdown) in RH during complete diurnal cycle except for a short period (around the peak temperature time of the day) in the late afternoon where it came close to the pre-lockdown value. Whereas in 2020, the variation in RH has been slightly different. It has been very close to pre-lockdown and during the night and the difference gradually increased during the day time as the temperature increased.

When compared quantitatively between 2019 and 2020 (Fig. 1(b)), T, ABL height and WS have shown decrease from 2019 to 2020 in both pre-lockdown and lockdown periods. All the comparative differences with the mean values for different parameters have been summarized in Table 2. Considering the fact that these are model reanalysis data sets (with significant uncertainty), and the observed changes falling within the standard deviation (Table 2) it can be assumed that meteorological conditions have been comparable in spite of differences between 2019 and 2020. Comparable meteorological parameters have also been reported by other studies during COVID-19 lockdown over India (Navinya et al., 2020; Sharma et al., 2020; Singh et al., 2020).

3.2. Impact of lockdown on trace gases (NO, NO_2, CO, O_3, SO_2, CO_2 and CH_4)

Fig. 2 shows the phase-wise statistical distribution of observed trace gas concentrations for the years 2019 and 2020. Time series of the trace gases (for 2019 and 2020) during the measurement period has been shown in Supplementary Fig. S2. In general most of the trace gas species have shown significant reduction during the lockdown period. In the pre-lockdown period the differences (compared to 2019) for NO, NO_2, CO_2, and CH_4 have been comparable with 2019 (<3% change) except for CO, O_3 and SO_2. CO has shown an increase (~9%) whereas O_3 has shown slight decrease (~5%) and SO_2 has shown substantial decrease (~40%). In the Phase I (when strict restrictions on all the non-essential activities have been on) all the other trace gases except CO_2 and CH_4 have shown a significant decrease. Quantitatively the reductions for NO, NO_2 and SO_2 have been in excess of 50%, for CO and O_3 have been in excess of 8% while CO_2 and CH_4 have shown the increase of 1–2%. Similar trend continued NO, NO_2, SO_2, CO_2 and CH_4 in the Phase II but CO reduced by 3.8%, whereas O_3 increased by 9.8%. O_3 showed a substantial increase in its concentration. Phase III has seen the decrease in all the trace gases. Even though CO_2 and CH_4 decreased but the decrease has been negligible. In the Phase IV, when many relaxations have been allowed, the concentrations of most of the gases (except NO, SO_2) increased, leading to reduction in the percentage difference. Overall, during the lockdown all the short lived species (dominated by anthropogenic emissions) have shown the substantial reduction in their concentration while long lived more stable species such as CO_2 and CH_4 have shown minimal difference.

NO_2 concentrations obtained over the Gadanki region from the Aura OMI satellite have also shown similar variations. Supplementary Fig. S3 (a) shows the statistical variations of OMI NO_2 for the years 2019 and 2020 during pre-lockdown and at different lockdown phases (I-IV). The changes from 2019 to 2020 in OMI NO_2 data have been −18.9%, −33.6%, −30.2%, −28.5%, −39.2% and −30.2% for pre-lockdown, Phase I, Phase II, Phase III, Phase IV and lockdown period, respectively. It is worth to recall that both these independent observations show similar decreasing trends in the concentrations. Satellite measurements of NO_2 cannot be compared directly with ground measurements, as the former is the area averaged concentration for the complete tropospheric altitudes whereas the latter is for the surface. Further, the discrepancies between the surface measurements and satellite observations can be expected due to the differences in the way they are obtained. Thus, only qualitative comparison has been made. All the observed quantitative changes in trace gases have been summarized in Table 3.

3.3. Impact of lockdown on aerosol parameters (PM_1, $PM_{2.5}$, PM_{10}, BC and AOD)

Fig. 3 shows the phase-wise changes in PM_1, $PM_{2.5}$, PM_{10}, BC and AOD. Time series of BC, AOD (for 2019 and 2020), and PM (only 2020) during the measurement period has been shown in Supplementary Fig. S4. There have been significant reductions in BC, AOD, and PM during the lockdown period in 2020. When compared with 2019 (phase-wise), BC showed the changes in the range of −65% to +24%. There has been an increase for BC in the pre-lockdown period but during lockdown BC has reduced. Like in trace gases, BC also showed the maximum decrease in Phase III of the lockdown and the difference decreased in the Phase IV. AOD obtained from the sky radiometer measurements showed the decrease in all phases. Phase-wise AOD changes have been in the range of −5% to –55%. AOD has also shown the maximum change in Phase III of the lockdown and difference reduced significantly in the Phase IV. Supplementary Fig. S3 (b) shows the comparison of AOD obtained for the Gadanki region from the MODIS satellite during 2019 and 2020. The variations have been different from the surface measurements in different phases. The changes at different phases have been in the range from −49% to +23%. Trend in Phase I, III, IV and lookdown has been similar like surface measurements (negative) but pre-lockdown period

Table 2
Summary of changes in meteorological parameters during the pre-lockdown and lockdown period and, comparison of the same with 2019.

Parameter	2020			2019			% Difference when compared to 2019		
	Pre Lockdown	Lockdown	% Difference	Pre Lockdown	Lockdown	% Difference	Pre Lockdown	Lockdown	Difference In Difference (approx. %)
Temperature (^{0}C)	25.7 ± 1.6	28.7 ± 1.3	+11.7	27.5 ± 1.5	31.3 ± 1.7	+13.8	**−6.5**	**−8.3**	−2.1
Relative Humidity (%)	65.6 ± 7.9	62.4 ± 8.4	−4.9	58.8 ± 1.2	53.5 ± 1.2	−9.0	**+11.6**	**+16.4**	**+4.1**
ABL height (m)	742.1 ± 163.2	778.2 ± 209.4	+4.9	880.5 ± 214.0	952.9 ± 249.0	+8.2	**−15.7**	**−18.3**	−3.3
Wind Speed (m/s)	2.13 ± 0.49	2.0 ± 0.62	−6.2	2.35 ± 0.68	2.11 ± 0.81	−10.2	**−9.4**	**−5.2**	**+4.0**

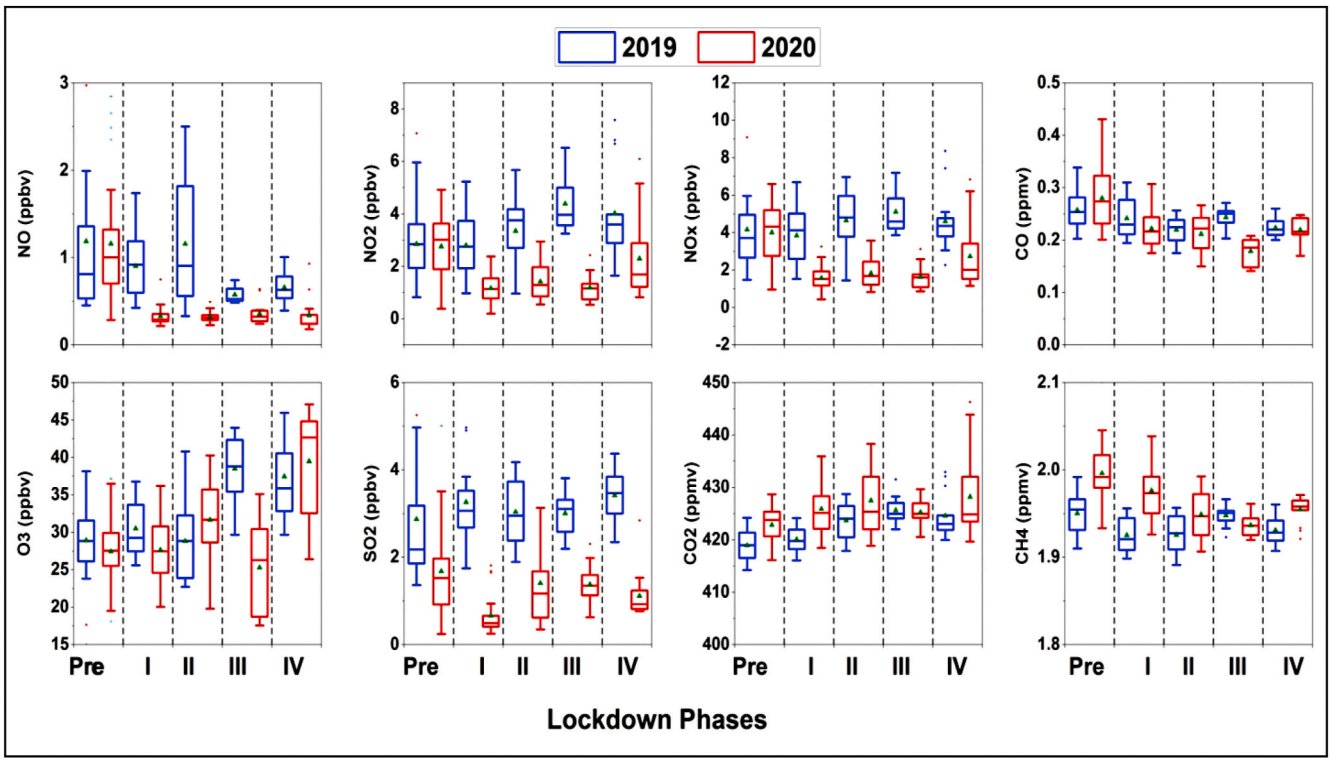

Fig. 2. Changes in the trace gas concentrations as the lockdown imposition extended from the first phase (Phase I, 25/03 to 14/04), to the second phase (Phase II, 15/04 to 03/05), third phase (Phase III, 04/05 to 17/05) and the IV Phase (Phase IV, 18/05 to 31/05).'Pre' represents the pre-lockdown period (15/02 to 21/03).

Table 3
Summery of the observed concentration changes during the pre-lockdown and lockdown period and comparison of the same with 2019. *Differences in NO might vary a little bit because NO concentrations have been very close to the detection limit of the instrument. There has been a significant change (qualitatively) but quantitative uncertainty may be little high. **PM differences have been calculated by taking the reference of pre-lockdown period because of 2019 data unavailability.

Sl. No.	Parameter	% change when compared to 2019					
		Pre Lockdown	Phase I	Phase II	Phase III	Phase IV	Total
	Dates ->	15/02–21/03	25/03–14/04	15/04–03/05	04/05–17/05	18/05–31/05	25/03–31/05
1	*NO	−0.6	−63.6	−72.4	−37.6	−48.1	−55.4
2	NO_2	−2.3	−58.3	−57.7	−72.9	−43.0	−58.0
3	NO_x	−2.4	−58.9	−60.7	−68.1	−40.5	−57.0
4	CO	+9.2	−8.2	−3.8	−26.6	−1.8	−10.1
5	O_3	−5.0	−9.4	+9.8	−34.3	+5.4	−7.1
6	SO_2	−40.7	−79.6	−53.6	−54.1	−67.3	−63.7
7	CO_2	+0.9	+1.4	+0.9	−0.1	+0.9	+0.8
8	CH4	+2.4	+2.6	+1.2	−0.6	+1.2	+1.1
9	BC	+24.1	−6.8	−43.6	−65.4	−21.0	−34.2
10	AOD	−6.2	−5.2	−21.3	−55.2	−9.7	−22.9
11	GHI	−0.7	+1.4	+1.9	+12.4	−3.8	+2.2
12	DHI	0.0	−6.6	−19.0	−7.6	+17.7	−4.1
13	Diffuse Fraction	0.0	+9.7	+18.2	+17	−20.9	−2.4
14	AOD (Modis)	+22.6	−17.3	+12.1	−49.2	−12.8	−16.8
15	NO_2 (OMI)	−18.9	−33.6	−30.2	−28.5	−39.2	−30.1
16	**PM_1	NA	−13.0	−45.0	−69.9	−35.0	−40.9
17	**$PM_{2.5}$	NA	−16.7	−52.0	−75.5	−42.7	−46.7
18	**PM_{10}	NA	−19.7	−56.3	−78.2	−47.2	−50.4

and Phase II values from the satellite data showed an increase. Despite high accuracy of ground-based AOD measurements, the spatial coverage is only possible through satellite retrievals. Recently, Madhavan et al. (2021) reported that the correlation between MODIS and Sky Radiometer AODs at Gadanki has improved significantly for different seasons but with a systematic underestimation of MODIS AOD as the magnitude of Sky Radiometer AOD increases. This underestimation has been attributed to the usage of less absorbing type aerosol model in the MODIS AOD retrieval (Kiran Kumar et al., 2013). Further, Sai Suman et al. (2014) indicated that a more absorbing aerosol model could replicate the fine mode aerosols while less absorbing model with coarse sea-salt particles as appropriate for coarse mode aerosols towards reducing the uncertainty in MODIS retrievals over Southern India.

Particulate matter data for 2019 has not been available (started November 2019) for the study period. Therefore pre-lockdown period has been considered as the reference as adopted by other studies (Shi and Brasseur, 2020). When compared with the pre-lockdown period with different phases of the lockdown, PM_1 changes have been in the range of −13% to – 70%, $PM_{2.5}$ showed the changes in the range −17% to −75% and PM_{10} in the ranges of −20% to −78%. Overall lockdown

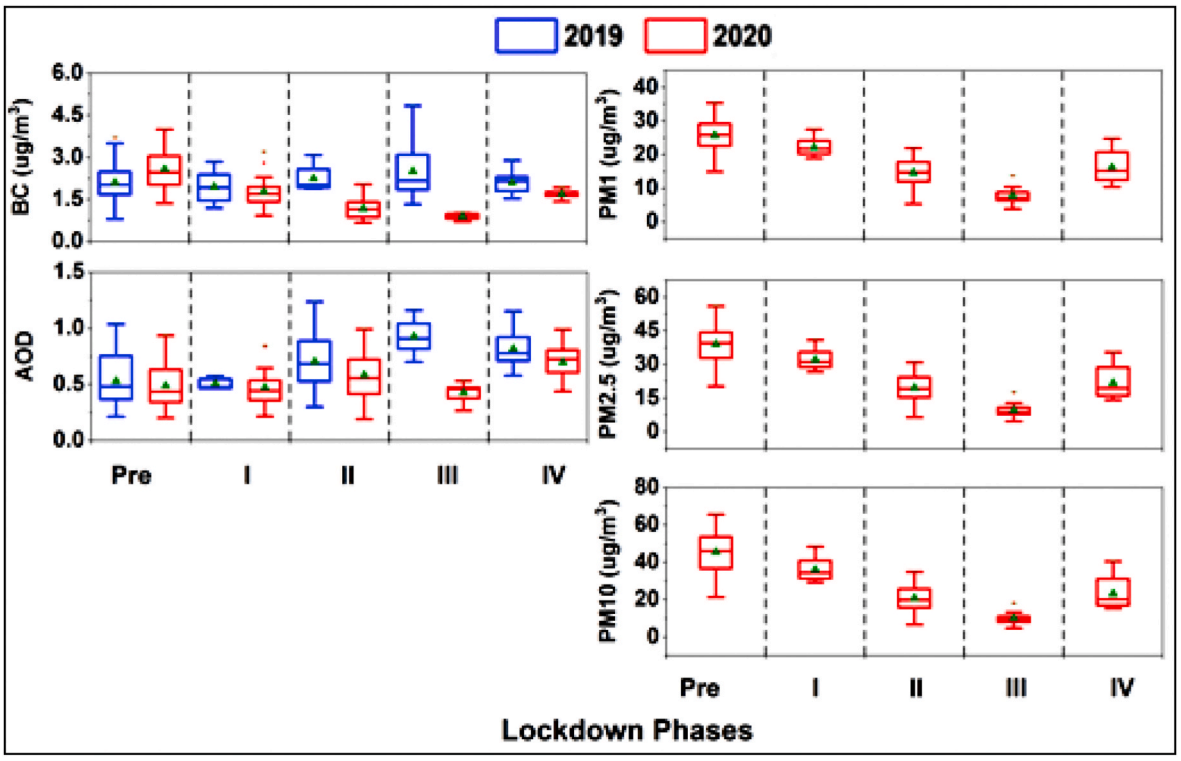

Fig. 3. Changes in BC and PM concentrations along with the observed AOD as the lockdown imposition extended from the first phase (Phase I, 25/03 to 14/04), to the second phase (Phase II, 15/04 to 03/05), third phase (Phase III, 04/05 to 17/05) and the IV Phase (Phase IV, 18/05 to 31/05). 'Pre' represents the pre-lockdown period (15/02 to 21/03). PM data is not available for 2019.

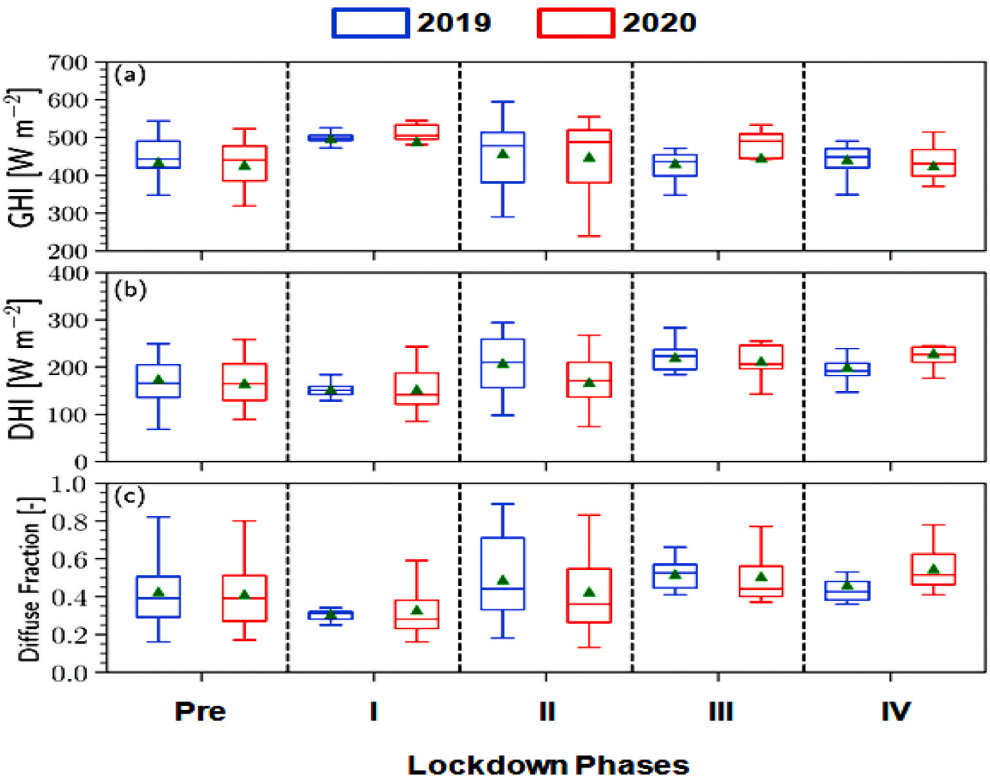

Fig. 4. Changes in GHI, DHI, and diffuse fraction (i.e., DHI/GHI) as the lockdown imposition extended from the first phase (Phase I, 25/03 to 14/04), to the second phase (Phase II, 15/04 to 03/05), third phase (Phase III, 04/05 to 17/05) and the IV Phase (Phase IV, 18/05 to 31/05). 'Pre' represents the pre-lockdown period (15/02 to 21/03).

period the changes in PM concentrations when compared to pre-lockdown phase have been −40.9%, −46.7%, and −50.4% for PM_1 $PM_{2.5}$ and PM_{10}, respectively. There has been a substantial decrease in the concentrations compared to the pre-lockdown phase in all the 3 PM. sizes. Like other atmospheric parameters Phase III has seen the highest decrease among the different phases. Phase-wise quantitative differences in aerosol parameters have been listed in Table 3.

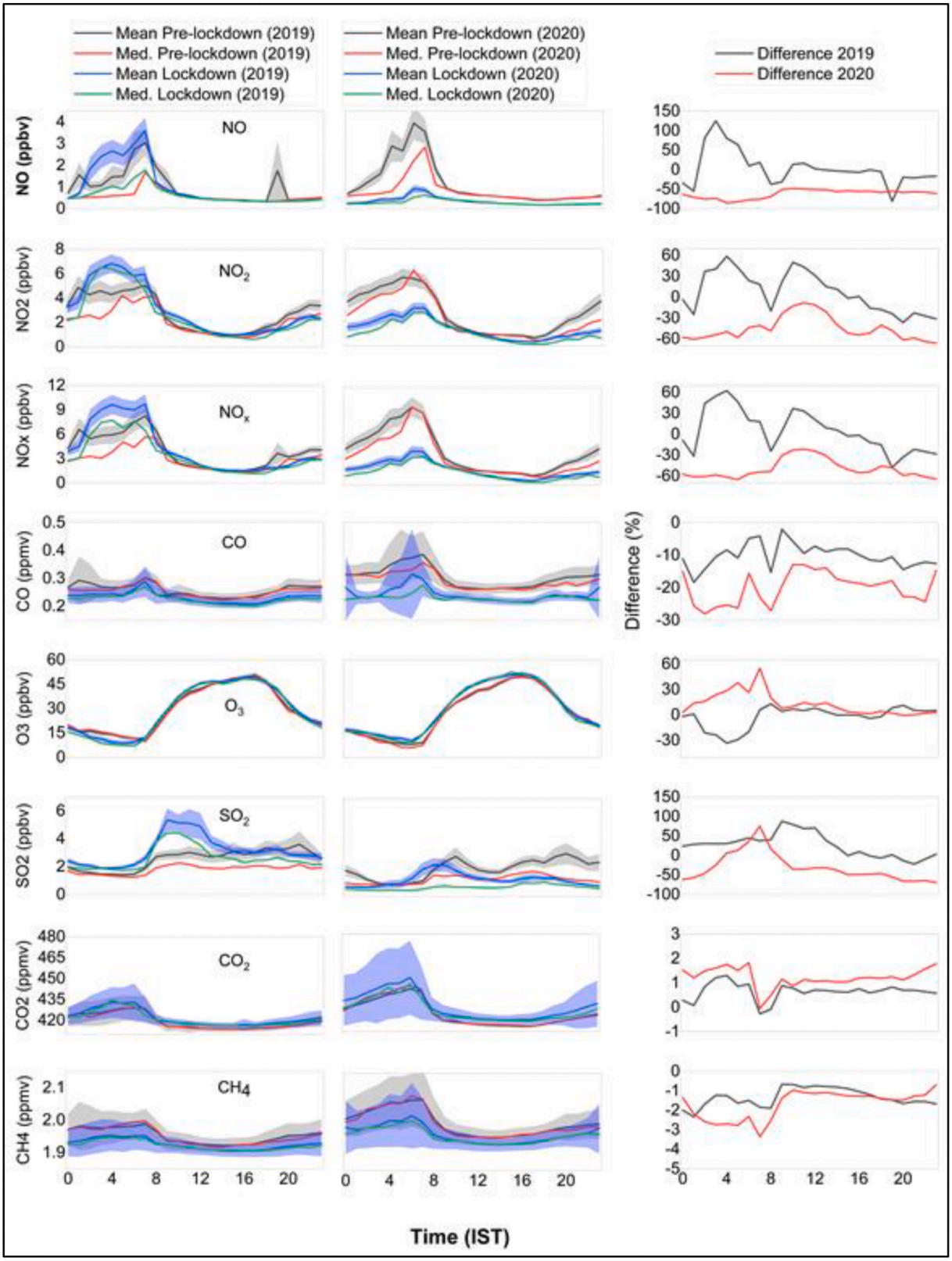

Fig. 5. Diurnal variations (averaged) of trace gases observed at Gadanki for the pre-lockdown (15/02 to 21/03) and lockdown (25/03 to 31/05) periods for 2019 and 2020. Differences represent the changes between the pre-lockdown and lockdown period for the corresponding years. Shaded area represents the stadard error.

3.4. Impact of lockdown on shortwave surface radiation

Shortwave downward radiation at the surface (or GHI) is a combination of direct solar beam component and diffuse component (or DHI) due to the scattering from atmospheric constituents and reflected from clouds. The statistical distribution of the daily mean GHI, DHI, and diffuse fraction (i.e., DHI/GHI) for different time periods of 2019 and 2020 is shown in Fig. 4. It should be noted that the diffuse fraction is an indirect measure of the sky condition. Higher diffuse fraction (~1.0) refers to overcast sky condition while the lower values (≤0.2) denote clear skies with stable background contribution representative of the observation location. Although the range of variability of GHI differs slightly, the median values have been observed to be comparable before the lockdown period for both 2019 (443 Wm^{-2}) and 2020 (440 Wm^{-2}). Similarly the range of variability and median values of DHI are found to be comparable before lockdown period for both 2019 (165 Wm^{-2}) and 2020 (164 Wm^{-2}). During the lockdown periods, the median values of GHI have been found to be higher by 7 Wm^{-2} (Phase I), 10 Wm^{-2} (Phase II), 51 Wm^{-2} (Phase III) in comparison with those in 2019. This is consistent with the observed decrease in DHI values by 10 Wm^{-2} (Phase I), 40 Wm^{-2} (Phase II), and 17 Wm^{-2} (Phase III) during 2020 in comparison with those in 2019. While the median of diffuse fraction has been the same (0.39) before lockdown period for both 2019 and 2020, there has been a considerable reduction of the diffuse fraction by 3% (Phase I), 8% (Phase II) and 9% (Phase III) in comparison with those in 2019. However, the phase IV lockdown period showed a reduction (~17 $W\ m^{-2}$) in median value of GHI during 2020 due to increased DHI (~35 $W\ m^{-2}$) and diffuse fraction (from 0.42 to 0.52). Further details on the observed relative change (%) in the GHI, DHI and diffuse fraction are given in Table 3.

3.5. Impact of lockdown on the diurnal variation of the pollutants

A more detailed diurnal analysis of the observed trace gases would help in better understanding of the changes occurred during the lockdown period. Most of the studies summarized in the introduction (of this article) focused on the overall changes in trace gas concentrations before and during the lockdown. However, there have been few studies which reported the diurnal changes too. To the best of our knowledge, there are two studies by Shi and Brasseur (2020) and Singh et al. (2020), where the authors have discussed the changes in the diurnal variations during the lockdown in Wuhan city China and over different regions of India, respectively. These studies showed the importance of diurnal variations while understanding the changes due to the lockdown. Fig. 5 shows the diurnal variations of trace gases (NO, NO_2, CO, O_3, SO_2, CO_2 and CH_4) for pre-lockdown and lockdown periods. There are striking differences in the diurnal variations. Overall reduction in the diurnal concentrations of the anthropogenic marker species like NO, NO_2, CO and SO_2 going from pre-lockdown to lockdown has been clearly captured. However, one has to be careful while looking into these changes because during the same period there will be the transition between winter season (Dec-Jan-Feb) to summer season at Gadanki (Mar-Apr-May) (Ratnam et al., 2008). This would potentially change the background conditions like, temperature, humidity and boundary layer altitude (Fig. 1). However, it has been observed there have been minimum differences in the meteorological parameters. To ensure that, the impacts of meteorological differences are taken care of the absolute difference between the pre-lockdown and lockdown have been calculated and inter-compared with previous year (2019) in the same time window. This would generally give us an approximate estimation of the background conditions impact and the changes above that would mean the changes due to the lockdown impact. Short-lived species like NO, NO_2, CO had shown the steady increase in their concentrations during the night before peaking in the early morning (07:00 IST) which is due to the fumigation effect when the boundary layer inversion takes place (Stull, 1988). This early peaking has also been evident in RH (Fig. 1) when the temperature and boundary layer inversion started. This effect has been predominant during the lockdown period in 2019. The steady increase in the concentration of these gases may be attributed to the more stable boundary layer (which results in poor mixing), lack of photo-chemistry and increased vehicular traffic. The highway connecting to Tirupati passing through Gadanki experiences increased night time traffic during summer time because of hot weather. Most of the heavy duty trucks prefer to run in the night time during this time of the year. Therefore one can expect an increase in the traffic marker species. Additionally this is the season when the school holidays start and Tirumala Temple is a famous Hindu pilgrimage (situated on the hill top in Tirupati) attracts more people visiting it. This induces an enhancement in personal vehicle traffic during this season. The effect has been clearly visible in the diurnal variations (2019) where the difference in the diurnal variations of pre-lockdown and lockdown time window has been mostly positive (except CO, which has been always negative, indicating the overall decrease in CO concentration from the per-lockdown period to lockdown) starting from the post-midnight hours (01:00–02:00 IST) until early morning (10:00–11:00 IST). After that when the photochemistry and increased boundary layer height (Fig. 1) came into effect, the difference shifted towards subzero. During the summer season Gadanki experiences more solar radiation and hence the hot weather, which increases the photochemistry as well as boundary layer expansion when compared to the pre-lockdown period. This effect lasted until midnight. Such a scenario has been completely changed during the year 2020. The differences of these species before and during the lockdown time never became positive and always stayed negative (%). The impact of these variations has also been transferred on the secondary species such as O_3. In 2019 the O_3 experienced a sharp decline in its concentrations in the early morning hours but such decline has never been observed in 2020 diurnal variations instead, O_3 steadily increased throughout the night and peaked during the early morning hours.

On the other hand SO_2 showed enhanced daytime increase in the concentrations during the lockdown time window in 2019, which may depend on many factors like local emissions (Datta et al., 2010; Lin et al., 2012). However, that day time increase has been significantly low during the lockdown period in 2020. SO_2 concentration peaks have been entirely different in 2020. SO_2 also showed a steady increase throughout the night and showing an early morning peak that had not been there in 2019.

Other more stable and long lived gases such as CO_2 and CH_4 have not shown any significant differences between 2019 and 2020 diurnal variation for the pre-lockdown and lockdown periods. Their diurnal variability has been mainly driven by the photochemistry and boundary layer dynamics. CO_2 has shown positive diurnal variation difference between the pre-lockdown and lockdown in all the hours (for both 2019 and 2020), and this difference has been higher in 2020. Along with the reduction in temperature during 2020 the increased CO_2 concentration might have partially induced the RH increase (Fig. 1) as there are reports stating that the positive feedback mechanism works for the CO_2 and H_2O relationship (Held and Soden, 2000). CH_4 has shown slightly lesser values during the night hours in 2020, day time variations have been comparable.

Fig. 6 shows the diurnal variations of BC and PM (1, 2.5 and 10). The difference in BC diurnal variations has been straight forward decreasing during the lockdown period in 2020. During 2019 pre-lockdown and lockdown time windows, diurnal variation has shown minimum percentage difference (close to zero) however that has been increased significantly towards the negative side in 2020. Like trace gas variations, a fumigation peak has been observed (in the early morning hours) in BC at all the times. The diurnal variation in BC has mainly been driven by the boundary layer expansion during day time resulting in lower day time concentrations (Ravi Kiran et al., 2018). Diurnal variation in PM (only for 2020) also showed similar features like BC and the differences between the pre-lockdown and during the lockdown has been significant (well below zero %).

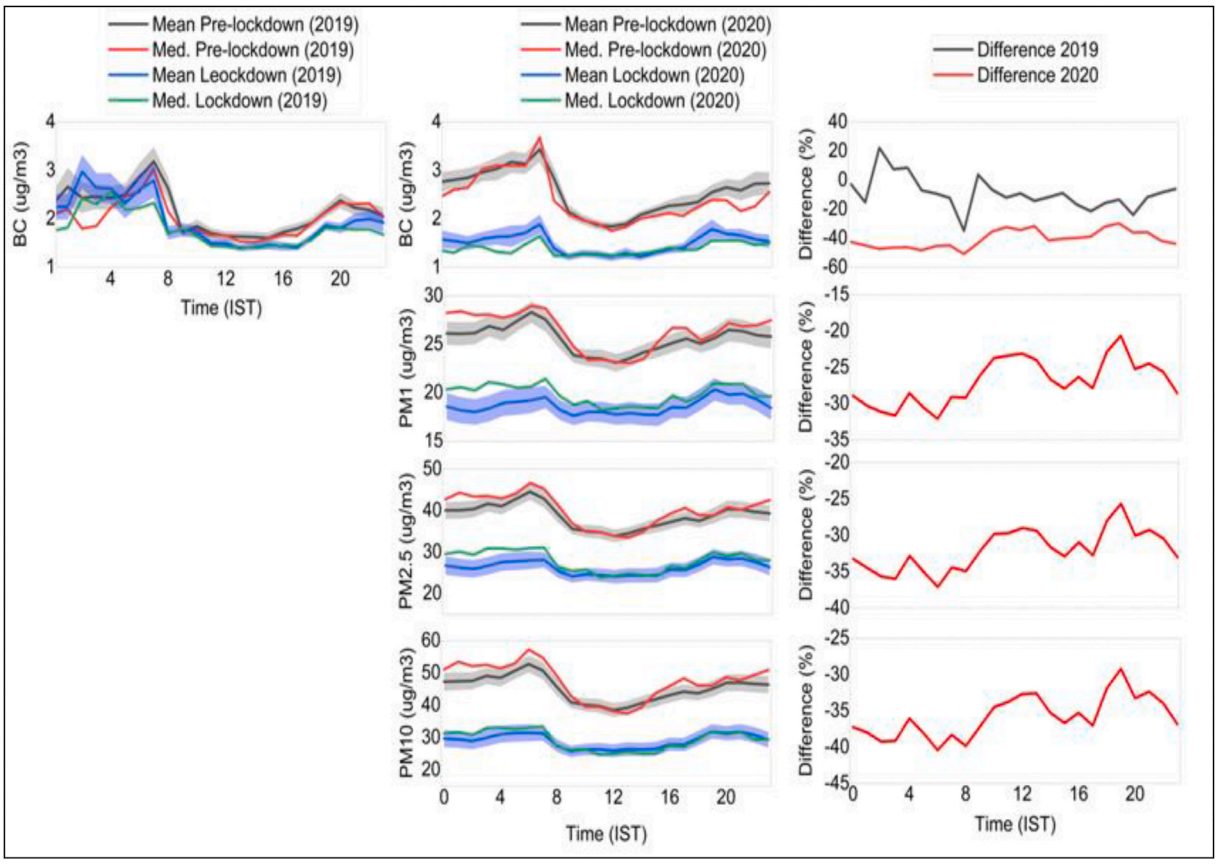

Fig. 6. Diurnal variations (averaged) of BC and PM observed at Gadanki for the pre-lockdown (15/02 to 21/03) and lockdown (25/03 to 31/05) periods for 2020. PM measurement data has not been available for 2019 therefore only Biswal et al. (2020) data has been compared. Differences represent the changes between the pre-lockdown and lockdown periods for the corresponding years. Shaded area represents the stadard error.

3.6. Impact of local and regional transport during the lockdown

To understand the local and regional transport impacts on the observed concentration changes during the pre-lockdown and lockdown periods, a three-day back trajectory clusters arriving at 500 m agl have been simulated using the NOAA global meteorological reanalysis data. After performing the cluster analysis, Concentration Weighted Trajectory (CWT) analysis has been performed using the TrajStat GIS based software extension to the HYSPLIT which is an useful tool for source identification (Wang et al., 2009). Results show that during the lockdown period local emission impacts have been more dominant compared to the transport. Therefore it may be inferred that the changes observed during the lockdown period at Gadanki have been induced by the changes in the local emission patterns. Fig. 7 shows an example CWT analysis for pre-lockdown and during the lockdown period performed on NO_x. Concentration weighing has been done on the trajectory clusters by taking the average concentrations observed during the pre-lockdown period and lockdown period to see the potential transport impacts on NO_X. A higher value in the average weighted concentration (color contour scale) of CWT implies that air parcels traveling over that particular trajectory cluster would be, on average, associated with high concentrations at the receptor (Wang et al., 2009).

4. Discussion

4.1. Composition changes

It is well understood that ambient concentrations of air pollutants are

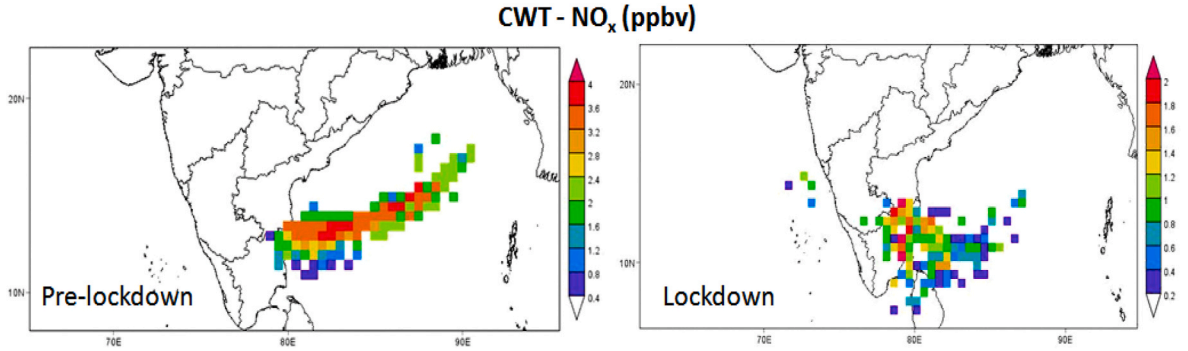

Fig. 7. Example results of Concentration Weighted Trajectory (CWT) analysis on NO_x during the pre-lockdown and lockdown periods showing the dominant local emission impacts on the observed concentration changes.

greatly affected by meteorology with low wind speeds causing a build-up of pollutants. Regional transport of the pollutants from the nearby regions also impacts the observed concentrations. Even though there have been small discrepancies in the meteorological conditions between 2019 and 2020, but they have been comparable. Absolute change wise (for the lockdown period in 2020) Temperature, ABL height and Wind Speed all have decreased while Relative Humidity increased (Table 2). These changes indicated more settled meteorological conditions which might have resulted in more stable atmospheric conditions. Therefore the changes observed in the concentrations have been mainly impacted by the emission changes rather than the meteorology. An evidence for this would be the negligible changes that have been observed in the stable species such as CO_2 and CH_4 (Table 3).

It is clear now that the lockdown has dramatically decreased the anthropogenic emissions and the impacts have been seen on the observed concentrations (Jain and Sharma, 2020; Mahato et al., 2020; Sharma et al., 2020; Shi and Brasseur, 2020; Singh et al., 2020; Wyche et al., 2021). As explained in section 3.1 and 3.2 most of the criteria pollutant concentrations responded negatively to the lockdown through their reductions. Allowed and restricted services/activities have been different during different phases of lockdown. Supplementary Table S3 lists all the services/activities that have been allowed or restricted in each phase of the lockdown (MHA, 2020). It is evident that Phase I and Phase II have been the strictest lockdowns and Phase III and Phase IV have seen various relaxations. Phase I and Phase II have seen maximum possible restrictions on traffic and industrial activities. These changes have been reflected in the observed concentrations but some of them have been delayed in response which extended to the Phase III and IV. Maximum changes (Table 3) have been in the Phase I and Phase II. Phase III also observed changes but there also have been rain events and the changes observed might have been the combined impacts. Most of the changes started reversing in Phase IV as more and more relaxations on anthropogenic activities have been given. Changes in the secondary species such as O_3 followed the NO_x variation during different phases.

AOD, BC and PM have also shown similar trends. PM concentration changes have been calculated by taking the pre-lockdown as the reference. Even though the meteorological parameters changed from pre-lockdown to lockdown, the observed changes in PM found to be beyond the changes potentially induced by the meteorological changes. Similar changes have been observed in other parameters (in this study) and other locations (Singh et al., 2020). Therefore, it can be assumed that observed PM changes have also been directly linked to the emission changes and the results confirm the same. The absolute reduction in fine mode particles ($PM_{2.5}$) has been higher (~18 μg/m^3) compared to the coarse mode particles (PM_{10}-$PM_{2.5}$) (~1.8 μg/m^3). Further, significant reductions in BC changes (2.5 μg/m^3 → 1.2 μg/m^3) have also confirmed that the reductions have been more on finer particles. These findings indicate that the changes observed might have been the result of the reductions in primary pollutant emissions (which have an intrinsic link with the Secondary Organic Aerosol (SOA) formation) due to lockdown anthropoause.

There has been an overall increase (~2%) in GHI and decrease in DHI (~4%). These changes can be significantly influenced by atmospheric aerosols, water vapour and clouds (e.g., Madhavan et al., 2017, 2016). Water vapour is highly variable in space and time with a strong absorption effect (mostly in the infrared beyond 0.9 μm) on the solar radiation components (GHI and DHI). Since water vapour is mainly concentrated in the lower atmosphere, it is considered as the second most important source of extinction of clear sky solar radiation after aerosols (Gueymard, 2014). Obregón et al. (2015) analysed the effect of water vapour content on the downward irradiance at the Earth's surface, and found that shortwave GHI reaching the surface increases when the water vapour content decreases. In contrast, increase of water vapour in the atmosphere eventually enhances the formation of cloud condensation nuclei and clouds which are able to reflect more incoming solar radiation (i.e., increase in DHI) and thus allowing less energy to reach the Earth's surface (i.e., decrease in GHI). Another possibility for increased DHI and diffuse fraction results from prevalence of the partly cloudy to overcast sky conditions. While clouds attenuate solar-radiation incidents on cloud shaded areas, sunlit ground surfaces may actually receive more GHI than under a clear sky due to light scattering and reflection from neighbouring clouds (i.e., broken cloud effect). Under thin high cloud conditions, GHI can be higher due to the dominance of DHI. Therefore, the temporal characteristics of GHI and DHI change significantly due to strong regional influences of changing cloud amounts, water vapour, and air quality (or emissions). Overall, it has been clearly evident that the observed increase in GHI and decrease in DHI and diffuse fraction have been a resultant of reduction in emission sources due to strict lockdown norms, decreased cloud cover, and intermittent rain events during Phases I, II and III. However the changes observed in the IV phase can be attributed to the increased cloudy conditions and possibly to the partial relaxation of the norms of the lockdown for essential services.

The changes observed at Gadanki have been within the range of changes reported by other studies. O_3 concentration changes have been mostly positive (up to 200%) (Lee et al., 2020; Nakada and Urban, 2020; Otmani et al., 2020; Sharma et al., 2020; Shi and Brasseur, 2020; Tobías et al., 2020). However, some studies reported the decrease (ranging between −39 and −7.5%) in the north-west, central and southern India (Jain and Sharma, 2020; Singh et al., 2020) and Wyche et al. (2021) have reported the O_3 decrease (ranging from −6% to −3.3%) in two rural sites in the UK. Gadanki O_3 change has been −7%. Other anthropogenic emission marker species like NO_2, NO, CO, SO_2, $PM_{2.5}$ and PM_{10} have also been in the range of changes observed in the above studies. A detailed comparison is given in the Supplementary Table S4.

4.2. Rural atmospheric chemistry

The atmospheric chemistry in the troposphere is driven by the two most powerful oxidants namely O_3 and OH radical (Prinn, 2003). They have close link among their formation and degradation in atmospheric conditions and both of them are controlled by solar radiation. O_3 is a secondary pollutant formed by its precursor's viz., nitrogen oxides (NO_x) and volatile organic compounds (VOC). Traffic is the main source (>50%) of O_3 precursors (Wayne, 2000). The formation mechanism for O_3 from nitrogen-dioxide (NO_2) (this is the most predominant way of its production in troposphere) can be given as,

$$NO_2 + h\upsilon\ (\lambda<420\ nm) \rightarrow NO + O(^3P) \quad R1$$

$$O(^3P) + O_2 + M \rightarrow O_3 + M \quad R2$$

where, M is a third body acting as an association complex stabilizer by collision. Above reactions are a part of cyclic reactions involved in the photochemical oxidation initiated by OH produced by O_3 and solar irradiation. On the other hand O_3 is also involved in the formation of OH vial following reactions.

$$O_3 + h\upsilon\ (\lambda<320\ nm) \rightarrow + O(^1D) + O_2(^1\Delta_g) \quad R3$$

$$O(^1D) + H_2O \rightarrow 2OH \quad R4$$

The OH radical chemistry in the troposphere is difficult to treat in isolation as it is closely associated with a reaction system involving HO_x (OH and HO_2), NO_x and O_3. In a relatively unpolluted environment (low NO_x regimes, which is the case with Gadanki) (Jain et al., 2019) reactions with CO and CH_4 become the main sinks of OH radicals (Monks, 2005; Seinfeld and Pandis, 2006) as given in the following reactions.

$$CO + OH \rightarrow H + CO_2 \quad R5$$

$$H + O_2 + M \rightarrow HO_2 + M \quad R6$$

$$HO_2 + NO \rightarrow NO_2 + OH \quad R7$$

$CH_4 + OH \rightarrow CH_3 + H_2O$ R8

$CH_3 + O_2 + M \rightarrow CH_3O_2 + M$ R9

CH_3O_2 (or generally termed as organic peroxy radicals) regenerate the OH through a similar reaction like R7 and also produce NO_2 which further takes part in the O_3 formation via R1 and R2. Therefore O_3 formation is always decided by the availability of two precursor species NO_2 and VOCs. The ratio between them decides the formation of O_3 and if the ratio is imbalanced (generally explained by the O_3 isopleths (Seinfeld and Pandis, 2006; Wayne, 2000)) then it ends up with a situation called NO_x limited regime (rural environments) or VOC limited regime (urban environments). Therefore, O_3 production is non-linier with the precursors (Chen et al., 2020; Renuka et al., 2014). In the environments where NO concentrations are high (urban environments), NO can act as the sink for O_3 via following reaction.

$NO + O_3 \rightarrow NO_2 + O_2$ R10

If the NO concentrations are low, one of the major sinks of O_3 is reduced and is the main reason for the observed higher O_3 concentrations in the rural environments. NO has a very short lifespan (a couple of minutes) and is immediately oxidized into NO_2 (Wayne, 2000), which has a longer lifespan of hours to even days, which allows it to be transported to different environments. Therefore any changes in NO_x concentrations would directly impact the chemical transformations involving formation and degradation of O_3 through reactions R1 and R2, and also enhance the reactivity of CO with OH radicals.

Gadanki is a rural site with a lot of vegetation around in the Eastern Ghats mountain range and agriculture fields. This means there is a VOC rich and NO_x limited zone for O_3 formation. Any increase in the NO_x should lead to the more O_3 production (up to the extent where the NO_x/VOC ratios cross over and NO becomes the sink for O_3) and any decrease in NO_x would generally expect to impact the O_3 negatively (Wyche et al., 2021). The same has been observed during the lockdown period (Table 3). When the traffic emission reduced during the lockdown that resulted in the reduction of both NO and NO_2 (Fig. 2, Table 3), even in rural environment (Biswal et al., 2020) leading to the reduction of O_3. This is in contrast with the other studies reporting the increase of O_3 in urban and polluted environments (Jain and Sharma, 2020; Mahato et al., 2020; Sharma et al., 2020; Shi and Brasseur, 2020; Singh et al., 2020; Xu et al., 2020a; Zambrano-Monserrate et al., 2020). In the urban environments which are NO_x rich, reduction of NO would have decreased the O_3 scavenging via R10 (change in the sink), but in rural environments which are VOC rich and NO_x limited any further reduction will only lead to the reduction of O_3 (change in the source) as shown by Singh et al. (2020) for southern part of India. Comparison of diurnal variations (Fig. 5) observed for O_3 and NO and NO_2 during the lockdown between 2019 and 2020 gives an excellent demonstration of the O_3 formation and degradation phenomenon observed at the site. In the 2019 case as the accumulation of the NO and NO_2 happened during the night (increased night time heavy duty vehicular traffic) and lack of photochemistry, the O_3 experienced a sharp decline in its concentrations when the NO and NO_2 concentrations have been at their highest (early morning hours). However, such decline has never been observed in 2020 diurnal variation, O_3 steadily increased throughout the night and peaked during the early morning hours. This demonstrates the lack of scavenging of O_3 by NO because of lower accumulation of NO during the night time when compared with the same period in 2019.

To understand the complete formation and loss processes of O_3 during the lockdown it may be required to have comprehensive non methane hydrocarbon (NMVOCs) data sets. Unfortunately VOC data sets have not been available for the study period and hence it is difficult to conclusively decide on the potential O_3 scavenging through VOC reactions. To have the O_3 scavenging through its reaction with VOCs, VOC/NO_x ratio should decrease significantly (Stockwell et al., 2011). Gadanki being a rural site (VOC rich environment) biogenic VOCs dominate the anthropogenic VOCs (Benzene, Toluene and Xylene etc.). Since the reductions observed during the lockdown have been mainly due to the anthropogenic emission changes, it can be assumed that, biogenic VOC concentrations remained the same during the lockdown even though the NO_x concentrations reduced significantly. These changes would have increased the VOC/NO_x ratio, and lead to the O_3 formation (Monks, 2005; Stockwell et al., 2011). However this increase would not have been dominant because the impact of NO_x change was expected to be very small (owing to their overall low concentration - NO_x limited regime). Therefore the changes observed in O_3, would go more with the O_3, NO and NO_2 photo-stationary state ($[O_3]=J_{NO2}[NO_2]/k[NO]$). Fig. 8 further confirms the photochemical repartition, total oxidant concentrations ($O_x=NO_2+O_3$) over the 2020 period have not been changed significantly as a result of the lockdown. The preservation of total O_x species observed here is the result of well-known tropospheric NO_x-O_3 photochemistry (Monks, 2005; Stockwell et al., 2011) as explained above. O_3 reduced to its lowest when NO_2 concentration has been least (Phase III) and increased to the maximum in Phase II when observed NO concentration has been at its lowest.

HONO chemistry in the troposphere also plays an important role in the formation and removal of O_3 (Monks, 2005; Wyche et al., 2021). HONO is mainly formed by the heterogeneous reaction of water with NO_2 and a minor portion by the reaction of NO_2, H_2O on the particles (this could account only for maximum 10% of NO_2 loss). HONO can also be emitted in small quantities by automobiles (Wayne, 2000). When photolysed during the early morning hours it produces OH and NO and, would influence the NO_x and OH budget (Jain et al., 2011a). However this pathway is significant only in polluted urban environments (could be up to 40–50% of the total OH formed) and insignificant in cleaner rural environments (could produce a maximum of 10%) like Gadanki. Therefore processes involving HONO might not have impacted much of the chemical changes observed during the lockdown at Gadanki.

Some studies (Li et al, 2019a, 2019b) have reported that particulate matter has the scavenging effect on HO_x and NO_x radicals (which would otherwise proceed to produce O_3) particularly in summer time. It has been observed that PM concentration too decreased significantly during the lockdown. This would go in favor of O_3 production. However, at Gadanki O_3 decrease because of non-availability of NO_2 looks to be the dominant path than the phenomena which are favoring production and sustainability (scavenging by NO) of O_3. Therefore, the net result observed has been the decrease of O_3. During the lockdown period in 2020 a slight increase (+2.2%) has been observed in GHI (Fig. 4, Table 3). Any increase in incoming shortwave radiation would increase

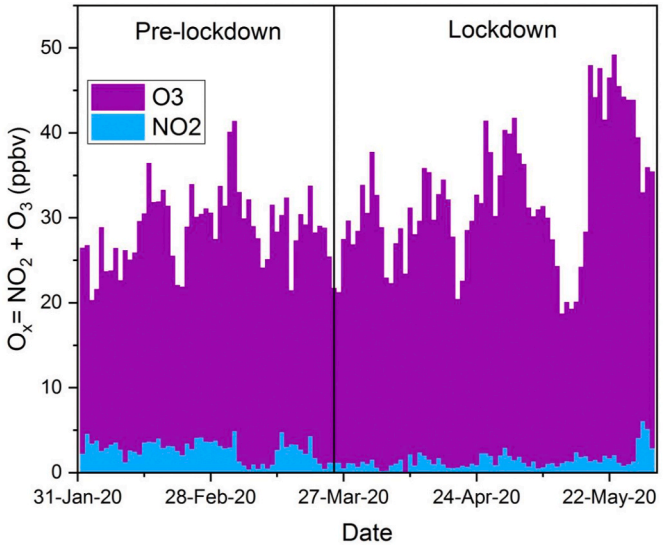

Fig. 8. Total daily O_x (NO_2+O_3) using stacked daily averages. Black line indicates the start of the India lockdown.

the efficiency of O_3 formation; however, the observed change has been very small and would not have induced significant changes in O_3 concentration.

Unlike 2019, 2020 lockdown period CO variations followed the NO_x (Fig. 2) indicating that, when the NO_x concentrations decreased CO became the main sink of OH through the reaction R5. This would add to the reduction of CO along with its reduced emissions because of lockdown restrictions. Therefore, net result has been enhanced reduction of CO during the lockdown and the effect would have also been transferred to the O_3 formation and degradation mechanisms.

A considerable decrease in SO_2 during 2020 when compared to 2019 has been observed both in pre-lockdown as well as the lockdown time. SO_2 primary sources are anthropogenic sources (Cox and Mulcahy, 1979; Garland, 1978; Wayne, 2000) and when the lockdown imposed most of the anthropogenic activities have been stopped resulting in the reduction of SO_2 emissions. However, SO_2 is also removed by both homogeneous and heterogeneous oxidation pathways in the boundary layer. All the removal processes convert SO_2 to H_2SO_4 (Jain et al., 2011b). Homogeneous oxidation linked with photochemistry is generally initiated with the reaction with OH radicals and then with H_2O to form H_2SO_4. However, OH production through O_3 photolysis is the dominant source of OH under study conditions and there has been a decrease of O_3 overall during the lockdown period. This should ideally reduce the photochemical sink of SO_2 and SO_2 should increase. Reactions involving other species such as peroxy radicals are rather slow and in polluted environments reaction with methyl peroxy (CH_3O_2) radical may become the significant sink. However, considering Gadanki is an unpolluted rural environment this pathway may not be accounted for SO_2 loss. O_3 reaction with SO_2 is also very slow and insignificant under the study conditions. Therefore, photochemical reduction which would be accounted for SO_2 change might not have been significant. Other dominating pathway of SO_2 removal in the boundary layer is through dry and wet deposition processes. Wet and dry deposition rates are 5–10 times higher than the homogeneous oxidation indicating the heterogeneous pathways are more dominating compared to homogeneous oxidation pathways (Wayne, 2000). Meteorological conditions such as RH, cloudiness and fog control the homogeneous and heterogeneous process. Higher RH enhances the oxidation rates indicating the more efficient removal of SO_2 (Liu et al., 2017). This could be one of the reasons along with anthropogenic emissions for the differences observed in 2020 because the RH has been higher by 11.5% during the pre-lockdown and 16.5% (Table 2) during the lockdown period. Higher relative humidity could have induced the faster removal process and hence the decrease in SO_2 concentrations. A study by Ye et al. (2018) reported the enhanced Secondary Organic Aerosols (SOA) formation from ozonolysis products of biogenic VOCs in SO_2 rich conditions. They have observed an enhancement in heterogeneous uptake of SO_2 at RH levels more than 50%. Additionally, recent studies also reported the enhanced SOA formation because of O_3 increase during the lockdown (Chatterjee et al., 2021). However, decrease in both O_3 and SO_2 have been observed at Gadanki. VOC data unavailability again makes it difficult to conclude the above path as one of the paths SO_2 removal and a source for secondary aerosols formation. However, it might have partially played a role in SO_2 reduction and hence SOA observed at Gadanki.

Almost all the studies on COVID-19 lockdown impact (Singh et al., 2020a, Bashir et al., 2020; Jain and Sharma, 2020; Mahato et al., 2020; Nakada and Urban, 2020; Navinya et al., 2020; Sharma et al., 2020; Xu et al., 2020a) reported a statistically significant improvement in the air quality during the COVID-19 lockdown. However, there has not been any change in the air quality category at Gadanki. Gadanki being a rural site the Air Quality Index (AQI) (Kanchan et al., 2015) generally stays in the category of good (0–50) to satisfactory (51–100) depending on the season of the year. AQI of Gadanki will be decided by O_3 sub-index owing to its observed higher concentration in comparison with the other criteria pollutants considered for the calculation of AQI. There has been a slight decrease of O_3 concentrations (8 h maximum for calculating the AQI) during the lockdown (2 ppbv) when compared with the 2019. This has induced a decrease of AQI by 4 (from 93 to 89) but that would not change the AQI category, so it still stayed the same (satisfactory range) as 2019.

5. Summary and conclusions

Restrictions imposed to stop the spread of COVID-19 over India have given a unique opportunity to study the variations in different aerosol, radiation and trace gases and their associated chemistry at tropical rural environment Gadanki. A significant reduction has been observed during the COVID-19 lockdown in almost all the short lived species which are directly linked with the anthropogenic emissions. On the other hand, the effect has been minimal on the long lived more stable species such as CO_2 and CH_4. When compared phase-wise, Phase III had the highest reductions this may be partly due to the observed rain events that could have resulted in wet scavenging during that phase. Changes in the concentrations also had the significant impact on atmospheric chemistry focused on O_3. Chemical changes in the rural environment have given an excellent demonstration of formation and degradation mechanisms of O_3 in the tropical rural environment. The salient conclusions from the study can be drawn as.

a) Meteorological parameters obtained from ERA5 data for the study period have been comparable for 2019 and 2020 with slight differences. The absolute changes (observed for 2020) in T, ABL height, RH and WS have been −2.1%, +4.8%, −3.3% and +4.0% respectively.
b) Trace gases have shown a variation of −55.4%, −58.8%, −10.1%, −7.1%, −63.7%, +0.8% and +1.1% for NO, NO_2, CO, O_3, SO_2, CO_2, and CH_4, respectively, during the lockdown period when compared with 2019. Phase-wise changes have been at their maximum during the Phase III and the differences generally reduced in the Phase IV. NO_2 variations obtained from the OMI satellite have shown a difference of −30.2% during the lockdown period when compared to 2019.
c) Particulate matter (PM_1, $PM_{2.5}$, and PM_{10}), Black carbon and AOD have also shown significant variations between 2019 and 2020. BC and AOD have shown 34.2% and 22.9% reductions during the lockdown period. Once again reduction has been its maximum in Phase III. PM data for 2019 has not been available hence the variations have been calculated taking the pre-lockdown period as reference. When compared with pre-lockdown period, PM_1, $PM_{2.5}$, and PM_{10} have shown a reduction of 40.9%, 46.7% and 50.4% during the lockdown period, respectively. AOD obtained from MODIS satellite data has also shown a reduction of 16.8% during the lockdown period when compared with 2019.
d) Similar reduction during the lockdown has been observed in both the ground-based observations and the satellite-borne measurements (in NO_2 and AOD) suggesting that latter can be used in absence of former observations.
e) Increase in GHI with decrease in DHI and diffuse fraction during the lockdown phases I, II and III is a resultant of reduction in emission sources due to strict lockdown norms along with the decreased cloud cover and intermittent rain events, while the vice versa during the phase IV lockdown period can be attributed to the increased cloudy conditions and possibly to the partial relaxation of the norms of the lockdown for essential services.
f) There have been striking differences in the diurnal variation of different atmospheric parameters. There has been a predominant steady increase in the concentrations throughout the night in 2019 but in 2020 the steady increase has been minimized. All the atmospheric parameters have shown the fumigation peak in the early morning hours. There has been a maximum impact on O_3 diurnal variation. During the lockdown period in 2019 there had been a

sharp decline in the early morning (dawn) O_3 concentrations when the NO_x concentrations reached their maximum. Such decline in the O_3 concentrations has not been observed in 2020 showing the lack of NO scavenging effect on O_3.

g) Variations observed are explained on the basis of known atmospheric chemistry of the rural environments. Rural environments are NO_x limited zones and any further reductions in NO_x would reduce O_3 concentrations and the same has been observed. This is in contrast with the other studies reported on urban environments. Phase-wise changes in O_3 followed the NO_x concentrations. CO variations also demonstrated the known chemistry of the rural environment.

h) Although there have been significant reductions in all the pollutants they remained still in the same AQI category. Therefore, in contrast to the other reported studies over urban environments, there has not been any change in the air quality at Gadanki during the lockdown.

Overall, lockdown imposed to stop the spread of COVID-19 provided an excellent demonstration of rural atmospheric chemistry and its intrinsic links with precursor concentrations and dynamics.

Credit author statement

Chaithanya D. Jain: Conceptualization, Methodology, Visualisation, Data curation, Writing- Original draft preparation. B. L. Madhavan: Data Curation, Visualisation, Writing- Original draft preparation, Vikas Singh: Methodology, Visualisation, Data curation, Writing- Reviewing and Editing, P. Prasad: Data curation, Writing- Reviewing and Editing, A. Sai Krishnaveni: Data curation, V. Ravi Kiran: Writing- Reviewing and Editing M. Venkat Ratnam: Resources, Visualisation, Supervision, Writing- Reviewing and Editing.

Declaration of competing interest

The authors declare that they have no known competing financial interests or personal relationships that could have appeared to influence the work reported in this paper.

Acknowledgements

We thank the Department of Space, Government of India for the financial support during this work through the ISRO-GBP ATCTM project. We also thank research scholars of ARTG (NARL) Ms. Sindu S. and Ms. Renju Nanadan for acquiring the data during the lockdown period. We acknowledge the use of TrajStat/HYSPLIT models for CWT studies. We thank ECMRWF-ERA5, NOAA-GRD, MODIS, OMI teams for the data used in the study. The data used in present study can be obtained on request.

Appendix A. Supplementary data

Supplementary data to this article can be found online at https://doi.org/10.1016/j.envres.2020.110665.

References

Bashir, M.F., Ma, B.J., Bilal, Komal, B., Bashir, M.A., Farooq, T.H., Iqbal, N., Bashir, M., 2020. Correlation between environmental pollution indicators and COVID-19 pandemic: a brief study in Californian context. Environ. Res. 187, 109652. https://doi.org/10.1016/j.envres.2020.109652.

Biswal, A., Singh, V., Singh, S., Kesarkar, A.P., Ravindra, K., Sokhi, R.S., Chipperfield, M. P., Dhomse, S.S., Pope, R.J., Singh, T., Mor, S., 2020. COVID-19 lockdown induced changes in NO_2 levels across India observed by multi-satellite and surface observations. Atmos. Chem. Phys. Discuss. 1–28. https://doi.org/10.5194/acp-2020-1023.

Chatterjee, A., Mukherjee, S., Dutta, M., Ghosh, A., Ghosh, S.K., Roy, A., 2021. High rise in carbonaceous aerosols under very low anthropogenic emissions over eastern Himalaya, India: impact of lockdown for COVID-19 outbreak. Atmos. Environ. 244, 117947. https://doi.org/10.1016/j.atmosenv.2020.117947.

Chen, Y., Beig, G., Archer-Nicholls, S., Drysdale, W., Acton, J., Lowe, D., Nelson, B.S., Lee, J.D., Ran, L., Wang, Y., Wu, Z., Sahu, S.K., Sokhi, R.S., Singh, V., Gadi, R., Hewitt, C.N., Nemitz, E., Archibald, A., McFiggins, G., Wild, O., 2020. Avoiding high ozone pollution in Delhi, India. Faraday Discuss. https://doi.org/10.1039/D0FD00079E.

Cox, R.A., Mulcahy, M.F.R., 1979. Photochemical oxidation of atmospheric sulphur dioxide [and discussion]. Philos. Trans. R. Soc. Lond. Ser. Math. Phys. Sci. 290, 543–550.

Datta, A., Saud, T., Goel, A., Tiwari, S., Sharma, S.K., Saxena, M., Mandal, T.K., 2010. Variation of ambient SO2 over Delhi. J. Atmos. Chem. 65, 127–143. https://doi.org/10.1007/s10874-011-9185-2.

Gadhavi, H.S., Renuka, K., Ravi Kiran, V., Jayaraman, A., Stohl, A., Klimont, Z., Beig, G., 2015. Evaluation of black carbon emission inventories using a Lagrangian dispersion model – a case study over southern India. Atmos. Chem. Phys. 15, 1447–1461. https://doi.org/10.5194/acp-15-1447-2015.

Garland, J.A., 1978. Dry and wet removal of sulphur from the atmosphere. Atmos. Environ. 12, 349–362. https://doi.org/10.1016/0004-6981(78)90217-2, 1967, Proceedings of the International Symposium.

Gueymard, C.A., 2014. Impact of on-site atmospheric water vapor estimation methods on the accuracy of local solar irradiance predictions. Sol. Energy 101, 74–82. https://doi.org/10.1016/j.solener.2013.12.027.

Gulia, S., Shiva Nagendra, S.M., Khare, M., Khanna, I., 2015. Urban air quality management-A review. Atmospheric Pollut. Res. 6, 286–304. https://doi.org/10.5094/APR.2015.033.

Hansen, A.D.A., 2005. Magee Scientific The Aethalometer ™.

Harrison, R.M., 2018. Urban atmospheric chemistry: a very special case for study. Npj Clim. Atmospheric Sci. 1, 1–5. https://doi.org/10.1038/s41612-017-0010-8.

Held, I.M., Soden, B.J., 2000. Water vapor feedback and global warming. Annu. Rev. Energy Environ. 25, 441–475. https://doi.org/10.1146/annurev.energy.25.1.441.

Hersbach, H., Bell, B., Berrisford, P., Hirahara, S., Horányi, A., Muñoz-Sabater, J., Nicolas, J., Peubey, C., Radu, R., Schepers, D., Simmons, A., Soci, C., Abdalla, S., Abellan, X., Balsamo, G., Bechtold, P., Biavati, G., Bidlot, J., Bonavita, M., Chiara, G. D., Dahlgren, P., Dee, D., Diamantakis, M., Dragani, R., Flemming, J., Forbes, R., Fuentes, M., Geer, A., Haimberger, L., Healy, S., Hogan, R.J., Hólm, E., Janisková, M., Keeley, S., Laloyaux, P., Lopez, P., Lupu, C., Radnoti, G., Rosnay, P. de, Rozum, I., Vamborg, F., Villaume, S., Thépaut, J.-N., 2020. The ERA5 global reanalysis. Q. J. R. Meteorol. Soc. n/a. https://doi.org/10.1002/qj.3803, 1–51.

Horiba, 2020. Ambient - HORIBA [WWW document] (accessed 8.1.20). https://www.horiba.com/in/process-environmental/products/ambient/.

Jain, C., Morajkar, P., Schoemaecker, C., Viskolcz, B., Fittschen, C., 2011a. Measurement of absolute absorption cross sections for nitrous acid (HONO) in the near-infrared region by the continuous wave cavity ring-down spectroscopy (cw-CRDS) technique coupled to laser photolysis. J. Phys. Chem. 115, 10720–10728. https://doi.org/10.1021/jp203001y.

Jain, C., Schoemaecker, C., Fittschen, C., 2011b. Yield of HO2 radicals in the OH-initiated oxidation of SO2. Z. Phys. Chem. 225, 1105–1115. https://doi.org/10.1524/zpch.2011.0169.

Jain, C.D., Gadhavi, H.S., Wankhede, T., Kallelapu, K., Sudhesh, S., Das, L.N., Pai, R.U., Jayaraman, A., 2018. Spectral properties of black carbon produced during biomass burning. Aerosol Air Qual. Res. 18, 671–679. https://doi.org/10.4209/aaqr.2017.03.0102.

Jain, C.D., Madhavan, B.L., Ratnam, M.V., 2019. Source apportionment of rainwater chemical composition to investigate the transport of lower atmospheric pollutants to the UTLS region. Environ. Pollut. 248, 166–174. https://doi.org/10.1016/j.envpol.2019.02.007.

Jain, S., Sharma, T., 2020. Social and travel lockdown impact considering coronavirus disease (COVID-19) on air quality in megacities of India: present benefits, future challenges and way forward. Aerosol Air Qual. Res. 20, 1222–1236. https://doi.org/10.4209/aaqr.2020.04.0171.

Jayaraman, A., Venkat Ratnam, M., Patra, A.K., Narayana Rao, T., Sridharan, S., Rajeevan, M., Gadhavi, H., Kesarkar, A.P., Srinivasulu, P., Raghunath, K., 2010. Study of atmospheric forcing and responses (SAFAR) campaign: overview. Ann. Geophys. 28, 89–101. https://doi.org/10.5194/angeo-28-89-2010.

Kanchan, K., Gorai, A.K., Goyal, P., 2015. A review on air quality indexing system. Asian J. Atmospheric Environ. 9, 101–113. https://doi.org/10.5572/ajae.2015.9.2.101.

Kelly, K.E., Whitaker, J., Petty, A., Widmer, C., Dybwad, A., Sleeth, D., Martin, R., Butterfield, A., 2017. Ambient and laboratory evaluation of a low-cost particulate matter sensor. Environ. Pollut. 221, 491–500. https://doi.org/10.1016/j.envpol.2016.12.039.

Kipp, Zonen, 2020. Pyranometers - Kipp & zonen [WWW document] (accessed 8.1.20). https://www.kippzonen.com/ProductGroup/3/Pyranometers.

Kiran Kumar, T., Gadhavi, H., Jayaraman, A., Sai Suman, M.N., Vijaya Bhaskara Rao, S., 2013. Temporal and spatial variability of aerosol optical depth over South India as inferred from MODIS. J. Atmospheric Sol.-Terr. Phys. 94, 71–80. https://doi.org/10.1016/j.jastp.2012.12.010.

Le Quéré, C., Jackson, R.B., Jones, M.W., Smith, A.J.P., Abernethy, S., Andrew, R.M., De-Gol, A.J., Willis, D.R., Shan, Y., Canadell, J.G., Friedlingstein, P., Creutzig, F., Peters, G.P., 2020. Temporary reduction in daily global CO 2 emissions during the COVID-19 forced confinement. Nat. Clim. Change 1–7. https://doi.org/10.1038/s41558-020-0797-x.

Lee, J.D., Drysdale, W.S., Finch, D.P., Wilde, S.E., Palmer, P.I., 2020. UK surface NO_2 levels dropped by 42 % during the COVID-19 lockdown: impact on surface O_3. Atmos. Chem. Phys. Discuss. 1–27. https://doi.org/10.5194/acp-2020-838.

Li, K., Jacob, D.J., Liao, H., Shen, L., Zhang, Q., Bates, K.H., 2019a. Anthropogenic drivers of 2013–2017 trends in summer surface ozone in China. Proc. Natl. Acad. Sci. Unit. States Am. 116, 422–427. https://doi.org/10.1073/pnas.1812168116.

Li, K., Jacob, D.J., Liao, H., Zhu, J., Shah, V., Shen, L., Bates, K.H., Zhang, Q., Zhai, S., 2019b. A two-pollutant strategy for improving ozone and particulate air quality in China. Nat. Geosci. 12, 906–910. https://doi.org/10.1038/s41561-019-0464-x.

Lin, W., Xu, X., Ma, Z., Zhao, H., Liu, X., Wang, Y., 2012. Characteristics and recent trends of sulfur dioxide at urban, rural, and background sites in North China: effectiveness of control measures. J. Environ. Sci. 24, 34–49. https://doi.org/10.1016/S1001-0742(11)60727-4.

Liu, W., He, X., Pang, S., Zhang, Y., 2017. Effect of relative humidity on O3 and NO2 oxidation of SO2 on α-Al2O3 particles. Atmos. Environ. 167, 245–253. https://doi.org/10.1016/j.atmosenv.2017.08.028.

Madhavan, B.L., Deneke, H., Witthuhn, J., Macke, A., 2017. Multiresolution analysis of the spatiotemporal variability in global radiation observed by a dense network of 99 pyranometers. Atmos. Chem. Phys. 17, 3317–3338. https://doi.org/10.5194/acp-17-3317-2017.

Madhavan, B.L., Kalisch, J., Macke, A., 2016. Shortwave surface radiation network for observing small-scale cloud inhomogeneity fields. Atmospheric Meas. Tech. 9, 1153–1166. https://doi.org/10.5194/amt-9-1153-2016.

Madhavan, B.L., Krishnaveni, A.S., Ratnam, M.V., Ravikiran, V., 2021. Climatological aspects of size-resolved column aerosol optical properties over a rural site in the southern peninsular India. Atmos. Res. 249, 105345. https://doi.org/10.1016/j.atmosres.2020.105345.

Mahato, S., Pal, S., Ghosh, K.G., 2020. Effect of lockdown amid COVID-19 pandemic on air quality of the megacity Delhi, India. Sci. Total Environ. 730, 139086. https://doi.org/10.1016/j.scitotenv.2020.139086.

Manisalidis, I., Stavropoulou, E., Stavropoulos, A., Bezirtzoglou, E., 2020. Environmental and health impacts of air pollution: a review. Front. Public Health 8. https://doi.org/10.3389/fpubh.2020.00014.

MHA, 2020. Governement of India COVID-19 Lockdown Guidelines- MHA, No.40-43/2020-DM-I (A).

Monks, P.S., 2005. Gas-phase radical chemistry in the troposphere. Chem. Soc. Rev. 34, 376–395. https://doi.org/10.1039/B307982C.

Nakada, L.Y.K., Urban, R.C., 2020. COVID-19 pandemic: impacts on the air quality during the partial lockdown in São Paulo state. Brazil. Sci. Total Environ. 730, 139087. https://doi.org/10.1016/j.scitotenv.2020.139087.

Nakajima, T., Tonna, G., Rao, R., Boi, P., Kaufman, Y., Holben, B., 1996. Use of sky brightness measurements from ground for remote sensing of particulate polydispersions. Appl. Optic. 35, 2672–2686. https://doi.org/10.1364/AO.35.002672.

National Research Council, 1992. Rethinking the Ozone Problem in Urban and Regional Air Pollution. https://doi.org/10.17226/1889.

Navinya, C., Patidar, G., Phuleria, H.C., 2020. Examining effects of the COVID-19 national lockdown on ambient air quality across urban India. Aerosol Air Qual. Res. 20, 1759–1771. https://doi.org/10.4209/aaqr.2020.05.0256.

Obregón, M.A., Costa, M.J., Serrano, A., Silva, A.M., 2015. Effect of water vapor in the SW and LW downward irradiance at the surface during a day with low aerosol load. IOP Conf. Ser. Earth Environ. Sci. 28, 012009 https://doi.org/10.1088/1755-1315/28/1/012009.

Ogen, Y., 2020. Assessing nitrogen dioxide (NO2) levels as a contributing factor to coronavirus (COVID-19) fatality. Sci. Total Environ. 726, 138605. https://doi.org/10.1016/j.scitotenv.2020.138605.

Otmani, A., Benchrif, A., Tahri, M., Bounakhla, M., Chakir, E.M., El Bouch, M., Krombi, M., 2020. Impact of covid-19 lockdown on PM10, SO2 and NO2 concentrations in salé city (Morocco). Sci. Total Environ. 735, 139541. https://doi.org/10.1016/j.scitotenv.2020.139541.

Picarro, IncU., 2020. G2401 gas concentration analyzer | picarro [WWW document] (accessed 8.1.20). https://www.picarro.com/products/g2401_gas_concentration_analyzer.

Pisoni, E., Van Dingenen, R., 2020. Comment to the paper "Assessing nitrogen dioxide (NO2) levels as a contributing factor to coronavirus (COVID-19) fatality", by Ogen, 2020. Sci. Total Environ. 738, 139853. https://doi.org/10.1016/j.scitotenv.2020.139853.

Prede, 2020. POM-01 skyradiometer [WWW document] (accessed 8.1.20). https://prede.com/english/betu-pom-01.html.

Prinn, R.G., 2003. The cleansing capacity of the atmosphere. Annu. Rev. Environ. Resour. 28, 29–57. https://doi.org/10.1146/annurev.energy.28.011503.163425.

Ratnam, M.V., Babu, A.N., Rao, V.V.M.J., Rao, S.V.B., Rao, D.N., 2008. MST radar and radiosonde observations of inertia-gravity wave climatology over tropical stations: source mechanisms. J. Geophys. Res. Atmospheres 113. https://doi.org/10.1029/2007JD008986.

Ratnam, V., Prasad, P., Raj, S.T.A., Ibrahim, H., 2020. Effect of lockdown due to COVID-19 on the aerosol and trace gases spatial distribution over India and adjoining regions. Aerosol Air Qual. Res. 20 https://doi.org/10.4209/aaqr.2020.07.0397.

Ravi Kiran, V., Talukdar, S., Venkat Ratnam, M., Jayaraman, A., 2018. Long-term observations of black carbon aerosol over a rural location in southern peninsular India: role of dynamics and meteorology. Atmos. Environ. 189, 264–274. https://doi.org/10.1016/j.atmosenv.2018.06.020.

Renuka, K., Gadhavi, H., Jayaraman, A., Lal, S., Naja, M., Rao, S.V.B., 2014. Study of ozone and NO2 over Gadanki – a rural site in south India. J. Atmos. Chem. 71, 95–112. https://doi.org/10.1007/s10874-014-9284-y.

Safarian, S., Unnthorsson, R., Richter, C., 2020. Effect of coronavirus disease 2019 on CO2 emission in the world. Aerosol Air Qual. Res. 20 https://doi.org/10.4209/aaqr.2020.0.0151.

Sai Suman, M.N., Gadhavi, H., Ravi Kiran, V., Jayaraman, A., Rao, S.V.B., 2014. Role of coarse and fine mode aerosols in MODIS AOD retrieval: a case study over southern India. Atmospheric Meas. Tech. 7, 907–917. https://doi.org/10.5194/amt-7-907-2014.

Seinfeld, J.H., Pandis, S.N., 2006. Atmospheric Chemistry and Physics: From Air Pollution to Climate Change, second ed. John Wiley & Sons, Inc.

Sharma, S., Zhang, M., Anshika, Gao, J., Zhang, H., Kota, S.H., 2020. Effect of restricted emissions during COVID-19 on air quality in India. Sci. Total Environ. 728, 138878. https://doi.org/10.1016/j.scitotenv.2020.138878.

Shi, X., Brasseur, G.P., 2020. The response in air quality to the reduction of Chinese economic activities during the COVID-19 outbreak. Geophys. Res. Lett. 47, e2020GL088070 https://doi.org/10.1029/2020GL088070.

Singh, V., Singh, S., Biswal, A., Kesarkar, A.P., Mor, S., Ravindra, K., 2020. Diurnal and temporal changes in air pollution during COVID-19 strict lockdown over different regions of India. Environ. Pollut. 266, 115368. https://doi.org/10.1016/j.envpol.2020.115368.

Stockwell, W.R., Lawson, C.V., Saunders, E., Goliff, W.S., 2011. A review of tropospheric atmospheric chemistry and gas-phase chemical mechanisms for air quality modeling. Atmosphere 3, 1–32. https://doi.org/10.3390/atmos3010001.

Stull, R.B., 1988. An Introduction to Boundary Layer Meteorology. Atmospheric and Oceanographic Sciences Library. https://doi.org/10.1007/978-94-009-3027-8. Springer Netherlands.

Tobías, A., Carnerero, C., Reche, C., Massagué, J., Via, M., Minguillón, M.C., Alastuey, A., Querol, X., 2020. Changes in air quality during the lockdown in Barcelona (Spain) one month into the SARS-CoV-2 epidemic. Sci. Total Environ. 726, 138540. https://doi.org/10.1016/j.scitotenv.2020.138540.

Wang, S., Hao, J., 2012. Air quality management in China: issues, challenges, and options. J. Environ. Sci. 24, 2–13. https://doi.org/10.1016/S1001-0742(11)60724-9.

Wang, Y.Q., Zhang, X.Y., Draxler, R.R., 2009. TrajStat: GIS-based software that uses various trajectory statistical analysis methods to identify potential sources from long-term air pollution measurement data. Environ. Model. Software 24, 938–939. https://doi.org/10.1016/j.envsoft.2009.01.004.

Wayne, R.P., 2000. Chemistry of Atmospheres. Oxford University Press.

Wyche, K.P., Nichols, M., Parfitt, H., Beckett, P., Gregg, D.J., Smallbone, K.L., Monks, P. S., 2021. Changes in ambient air quality and atmospheric composition and reactivity in the South East of the UK as a result of the COVID-19 lockdown. Sci. Total Environ. 755, 142526. https://doi.org/10.1016/j.scitotenv.2020.142526.

Xu, K., Cui, K., Young, L.-H., Hsieh, Y.-K., Wang, Y.-F., Zhang, J., Wan, S., 2020a. Impact of the COVID-19 event on air quality in Central China. Aerosol Air Qual. Res. 20, 915–929. https://doi.org/10.4209/aaqr.2020.04.0150.

Xu, K., Cui, K., Young, L.-H., Wang, Y.-F., Hsieh, Y.-K., Wan, S., Zhang, J., 2020b. Air quality index, indicatory air pollutants and impact of COVID-19 event on the air quality near Central China. Aerosol Air Qual. Res. 20, 1204–1221. https://doi.org/10.4209/aaqr.2020.04.0139.

Ye, J., Abbatt, J.P.D., Chan, A.W.H., 2018. Novel pathway of SO_2 oxidation in the atmosphere: reactions with monoterpene ozonolysis intermediates and secondary organic aerosol. Atmos. Chem. Phys. 18, 5549–5565. https://doi.org/10.5194/acp-18-5549-2018.

Zambrano-Monserrate, M.A., Ruano, M.A., Sanchez-Alcalde, L., 2020. Indirect effects of COVID-19 on the environment. Sci. Total Environ. 728, 138813. https://doi.org/10.1016/j.scitotenv.2020.138813.

Zheng, T., Bergin, M.H., Johnson, K.K., Tripathi, S.N., Shirodkar, S., Landis, M.S., Sutaria, R., Carlson, D.E., 2018. Field evaluation of low-cost particulate matter sensors in high- and low-concentration environments. Atmospheric Meas. Tech. 11, 4823–4846. https://doi.org/10.5194/amt-11-4823-2018.